Stem Cell Research & Therapy

RESEARCH

Open Access

Astilbin improves the therapeutic effects of mesenchymal stem cells in AKI-CKD mice by regulating macrophage polarization through PTGS2-mediated pathway

Xiaodong Geng[1,3†], Zhangning Fu[1,2], Guangrui Geng[1,2,4], Kun Chi[1,2], Chao Liu[5], Haijuan Hong[6], Guangyan Cai[1,2], Xiangmei Chen[1,2] and Quan Hong[1,2*]

Abstract

Background Although mesenchymal stem cells (MSCs) have been proven to be appropriate candidates for the treatment of AKI-CKD, their efficacy is limited and variable. Astilbin (AST) had a protective effect on MSCs from oxidative stress via ROS-scavenging, however, whether it can improve MSCs' renoprotection and the underlying mechanism need to be elucidated.

Methods AST-pretreated MSCs were administered intravenously into the ischemia–reperfusion injury mice models and the renal function, pathological changes and inflammation. Were evaluated. In addition, DARTS, molecular docking, surface plasma resonance(SPR), dual-luciferase reporter gene assay and the ChIP-PCR were utilized to explore the potential signaling pathways through which AST exert renal protective effects on MSCs.

Results AST-pretreated MSCs markedly improved kidney function, reduced kidney pathological injury and inflammation in AKI and AKI-CKD mice. RNA-seq results showed that PTGS2 related pathway was significantly up-regulated in MSCs after AST pretreatment. DARTS assay, molecular docking and SPR assay revealed that AST could bind with the transcriptional factor of Kruppel-Like Factor 4(KLF4) protein. The promoter of PTGS2 had the binding and transcriptional activation by KLF4. Furthermore, AST pretreatment promoted the secretion of PGE2 in MSCs. And then the westren blot results showed that the protein levels of CD163 and CD206 were upregulated after coculture in AST-pretreated MSCs, indicating that the polarization of RAW264.7 cells towards M2-like macrophages was induced. Knockdown of PTGS2 reversed the ability of AST-pretreated MSCs in converting macrophages to M2 phenotype and reducing their therapeutic effects on AKI-CKD mice.

Conclusion AST pretreatment enhances the efficacy of MSCs on AKI and AKI-CKD mice by inducing of M2-like phenotype polarization in macrophages through the PTGS2-mediated pathway. This approach not only provides a novel strategy to strengthen the capability of MSCs but also helps elucidate the beneficial effects of the Chinese herbal medicine AST.

Keywords Astilbin, Mesenchymal stem cells, Macrophage polarization, AKI-CKD, PGE2

†Xiaodong Geng and Zhangning Fu contributed equally to this work.

*Correspondence:
Quan Hong
hongquan@301hospital.com.cn
Full list of author information is available at the end of the article

Background

Previous clinical studies have shown that acute kidney injury (AKI) predisposes to the development and progression of chronic kidney disease (CKD) [1, 2]. Identifying effective therapeutic interventions to treat AKI and prevent its progression to CKD is an urgent matter. Mesenchymal stem cells (MSCs)-based therapies have been demonstrated to be a promising strategy for AKI treatment [3, 4]. MSCs could improve the structural and functional recovery of AKI and these effects were thought to be attributed to their immunomodulatory and anti-inflammatory capabilities [5]. However, the efficacy of MSCs-based treatments are limited and variable [6]. To address this problem, several priming strategies including the use of cytokines and natural/chemical compounds, such as IFN-γ, TNF-α, melatonin, Darbepoetin-α(DPO) and IL-17A have been developed for some specific disease indications [7–9]. Pretreatments with these cytokines and compounds have been shown to enhance the immunomodulatory functions of MSCs and thereby facilitating their potential therapeutic efficacy [10–12]. Moreover, compounds are easier to synthesize and obtain compared to cytokines.

Astilbin (AST) is a type of flavonoid having multiple pharmacological properties including immunomodulatory, anti-inflammatory and antioxidant effects [13]. AST can be extracted from various plants such as Rhizoma Smilacis Glabrae and Sarcandra glabra. Numerous experiments on immunological diseases including systemic lupus erythematosus, arthritis, and psoriasis, have verified the immune-regulatory properties of AST [14]. Of note, AST has also been suggested to have the ability to protect MSCs from oxidative stress-induced apoptosis and help them exert antioxidant action by directly or indirectly scavenging reactive oxygen species (ROS) [15].

Therefore,we investigated the effects and mechanism of AST pretreated MSCs on the treatment of AKI-CKD. Our results indicated that AST enhanced the immunomodulatory functions of MSCs and attenuated AKI and AKI-CKD through PTGS2 (prostaglandin-endoperoxide synthase 2)-mediated pathway. This approach not only provides a novel strategy to strengthen the capability of MSCs in the treatment of AKI-CKD but also helps elucidate the beneficial effects of the Chinese herbal medicine AST.

Materials and methods

Cell culture

Human bone marrow MSCs were obtained from Cyagen Company (Guangzhou, China) and cultured in MSCs complete medium (HUXMA-90011; Cyagen). The mouse macrophage line RAW264.7 were purchased from ATCC company (Manassas, VA, USA) and cultivated in RPMI 1640 medium (Cat#C22400500BT, GIBCO) augmented with 10% foetal bovine serum. All cells were cultured in an incubator with 5% CO_2 at 37 °C.

Mice models and surgical procedure

All animal studies were approved by the Animal Ethics Committee of the Chinese PLA General Hospital. Male C57 BL/6 J mice (SPF Biotechnology Co.,Ltd) were used to established the AKI-CKD mice models. Mice were individually housed in captivity in the Experimental Animal Center with controlled temperature and light cycles (24 °C and 12/12 light cycle) and the study protocols adhere to the ARRIVE guidelines. Unilateral ischemia–reperfusion injury(IRI) plus contralateral nephrectomy mice models were generated by clamping the left renal pedicle for 35 min followed by clamp release to allow reperfusion. Contralateral kidney was removed prior to sample collection. MSCs (10^6 per mouse) were administered intravenously via the tail vein into the mice after reperfusion. The mouse were randomly divided into five groups as follows (n = 6 per group): the Sham group, the AKI group, the MSC group, the AST-MSC group,the AST-MSC-shRNA-PTGS2 group. MSCs or AST-pretreated MSCs were all washed three times in phosphate buffered saline before injection. Animals were anaesthetized by intraperitoneal injection of 2% (w/v) pentobarbital sodium solution (2.0 ml/kg) in order to minimalize the stress and suffering of animals. 15 min after administration of anaesthetics, animals were euthanized by the disruption of the spinal cord. Blood was harvested at Day 1, 3, 5, 7, 14, 21 and kidney was harvested at Day 3, 21 for further processing.

Measurements of serum creatinine (Scr) and blood urea nitrogen (BUN)

The levels of Scr and BUN were determined utilizing the Creatinine Assay Kit and Urea Assay Kit (QuantiChrom. BioAssay Systems) according to the manufacturer's instructions.

Enzyme-linked immunosorbent assay (ELISA)

The concentrations of IL-6, IL-10, TNF-α and PGE2 in the serum or MSC cells culture supernatant were quantified using ELISA (R&D Systems, Minneapolis, MN) in accordance with the manufacturer's instructions.

Histopathological assessment

Kidney tissues were fixed in 4% paraformaldehyde (PFA) for 24 h before standard dehydration and paraffin embedding. Renal tissues were sectioned at 3 μm and stained with periodic acid Schif (PAS) and Masson's trichrome using a standard protocol. The blind method was utilized to evaluate tubular damage in histological

examinations. 0 represents normal histology, and 1–4 represent ≤ 25%, ≤ 50%, ≤ 75%, and > 75% abnormal histology, respectively Image J was used to measure the area of light green-stained collagen fibers in Masson-stained kidney tissues.

RNA-sequencing (RNA-seq)

MSCs were seeded onto 6-well culture plates and allowed to grow for 12 h in a complete medium until 70% confluence was obtained. After that, the cells were incubated in a serum-free medium for 12 h to synchronize the cells. The normal cells were then subjected to routine culture media and treated with AST (20 μg/ml) for 48 h. Total RNA was collected using TRIzol reagent (Invitrogen, Grand Island, NY) for subsequent RNA-seq. The sequencing service used was LC-Bio Technology Co., Ltd. (Hangzhou, China). The sequencing data supporting the results are uploaded as supplementary materials.

Evaluation of drug affinity-responsive target stabilization (DARTS)

DARTS was utilized to identify target proteins that bind directly to small molecules. MSCs were grown to a confluence of 80–85%, and then washed with ice-cold PBS. 100 μL of M-PER lysis solution containing 1% protease and phosphatase mixed inhibitor was added to the cells and lysed on ice for 30 min. The total protein lysates were centrifuged at 12,000 rpm for 10 min at 4 °C. BCA protein concentration test was performed to assess the protein concentration of the supernatant. A total of 500 μg protein solution and 20 μg/ml AST were mixed and incubated at 4 °C for 12 h. Protease solutions were mixed with samples and incubated at room temperature for 30 min, after which the loading buffer was added to terminate the reaction. The resulting samples were analyzed by SDS-PAGE for subsequent western blot or LC–MS/MS examination.

Molecular docking

AST and its targeted proteins were chosen for molecular docking. The 2D structure of AST was retrieved from the PubChem database, and the 3D structures (X-RAY DIFFRACTION) of targeted proteins were downloaded from the RCSB PDB database in PDB format [16]. Autodock Vina was utilized for molecular docking [17, 18], and a docking score of less than 6.5 was deemed indicative of a potential binding affinity.

Surface plasmon resonance (SPR)

AST and protein binding was studied by the surface plasma resonance (SPR) measurement using Biacore X100 (GE Healthcare). Recombinant human KLF4 protein (ab169841, Abcam) was covalently coupled to a CM5 chip (Biacore, GE Healthcare). All data were collected at 25℃ with HBS-EP running buffer. Different dilutions of AST were passed onto the CM5 chip. The association rate constant ka and dissociation rate constant kd were calculated and analyzed by the Biacore evaluation software and the equilibrium dissociation constant (K_D) was calculated (K_D = kd/ka).

Chromatin immunoprecipitation (ChIP)

The ChIP-PCR procedure was performed as previously described [19]. In brief, ChIP DNA from anti-KLF4 (ab215036, Abcam)-treated human MSC cells was used to examine the association between KLF4 and PTGS2. DNA from anti-IgG antibody-treated cells was served as the control. Purified DNA was used to analyze the PTGS2 proximal promoter region by real-time PCR. The PTGS2 primers were as follows: forward: 5′-AAACTA GGACTGGCCCTTCA-3′; and reverse: 5′-TTCCAA CACAGTGTCGCAGT-3′(Homo sapiens). The relative amplification of the promoter sequence of the gene was calculated using the $2^{-\Delta\Delta}$CT method.

Dual-luciferase reporter assay

The wild-type human PTGS2 promoter, containing the potential binding site (− 1781 ~ − 1770 nt), was obtained by PCR amplification. The promotor was then subcloned into the pGL3-Basic vector (Promega, Madison,USA) and designated as pGL3-WT-PTGS2. Additionally, the binding site -GTCCCCACTCTC- within the PTGS2 promoter was mutated to -CATCGCGCCCTGCT- and named as pGL3-MT-PTGS2. Plasmid (pReceiver-M94) containing full-length human KLF4 cDNA was acquired from GeneCopoeia. Using Lipofectamine 2000, HEK293T cells were transfected with the KLF4 overexpression plasmid and either pGL3-WT-PTGS2 or pGL3-MT-PTGS2 depending on the strain of pGL3 they contained. The samples were then cotransfected with a pRL-TK (Promega) plasmid expressing Renilla luciferase. The luciferase activity levels of both Firefly and Renilla were evaluated using a dual-luciferase reporter assay system.

Transwell assay

MSCs were treated with or without AST (20 μg/ml; HY-N0509, MCE Corporation, USA) for 48 h. The cells were resuspended in PBS and subjected to in vivo/vitro analyses as AST-pretreated MSCs or control MSCs. To examine the effects of AST-pretreated MSCs on macrophage polarization, RAW264.7 and AST-pretreated MSCs were cocultured for 48 h in a Transwell system containing membranes with a pore size of 4 m in a 6-well plate, allowing free diffusion of molecules but not cell translocation between the two compartments.

shRNA-PTGS2 transfection

Short hairpin RNAs (shRNAs) to human PTGS2 (shRNA-PTGS2#1 and shRNA-PTGS2#2) and a scrambled control shRNA-NC were obtained from Sigma-Aldrich. PTGS2 expression plasmid LV-PTGS2 were procured from Miaolingbio (Wuhan, China), LV-NC was used as a control. Transfection with shRNA was performed with Lipofectamine 3000 (Invitrogen, L3000-015) according to the manufacturer's instructions. The following is the shRNA sequences used:

shRNA-PTGS2#1, 5'-GCTGAATTTAACACCCTC TAT-3' (Forward).

shRNA-PTGS2#2, 5'-CCGTACACATCATTTGAA GAA-3' (Forward).

Immunofluorescent staining

The expression of CD206 in paraffin-embedded slices of mice kidney tissues was assessed with CD206 monoclonal antibody (ab64693, Abcam). Heat-mediated antigen retrieval was conducted in citrate buffer (pH 6, epitope retrieval solution) for 10 min. The tissue sections were blocked with 10% goat serum and incubated with CD206 antibody at 4 °C overnight. Cy3-conjugated goat anti-rabbit IgG (A0516, Beyotime) was used as the secondary antibody at a 1:300 dilution. The sections were incubated in the secondary antibody at room temperature for 1 h, followed by counterstained with DAPI. The slides were imaged by confocal fluorescence microscopy (Olympus, Tokyo, Japan).

Western blot analysis

Proteins were extracted from cells or tissues using RIPA lysate, separated by electrophoresis on a 10% SDS–polyacrylamide gel, and then transferred to a polyvinylidene fluoride membrane for further analysis. The membrane was blocked with 5% skim milk at room temperature for 1 h before incubated with the following primary antibodies:

COX2 (66,351-1-Ig, Proteintech), F4/80 (ab300421, Abcam), CD163 (ab182422, Abcam), CD206 (ab64693, Abcam),α-SMA (55,135-1-AP, Proteintech), and Collagen Type III (22,734-1-AP, Proteintech). Goat anti-rabbit IgG (#ab205718, Abcam) conjugated with horseradish peroxidase was utilized as the secondary antibody. The blots were detected by enhanced chemiluminescence kit (Beyotime), and the gray values were analyzed by Image J software.

Statistical examination

All data are expressed as mean ± standard deviation (SD). Statistical analysis was performed using GraphPad Prism 8.21 software. Comparisons between groups were conducted using one-way analysis of variance (ANOVA), followed by Student's t-test. A value of $\mathbf{p} < 0.05$ was indicated statistical significance.

Results

MSCs pretreated with AST improved the renoprotective efficacy in AKI

To determine the optimal pretreatment condition for AST on MSCs, we evaluated the effects of prolonged AST treatment on the proliferation and viability of MSCs. Cells were treated with various concentrations (0, 5, 10, 20, 40, 80 μg/ml) of AST and monitored using the real-time cellular analysis (RTCA) system (Fig. S1A) and CCK8 assay (Fig. S1B). The results indicated that low concentrations of (5 and 10 μg/ml) AST had no effects on the growth and viability of MSCs within 48 h, whereas 20 μg/ml AST obviously enhanced the growth and viability of MSCs at 48 h. Intriguingly, with the increase of AST concentration to 40 μg/ml and 80 μg/ml, the proliferation and viability of MSCs were inhibited, suggesting that the optimal concentration and time point for AST pretreatment on MSCs are 20 μg/ml and 48 h. This pretreatment condition was applied in the subsequent experiments.

We next examined the effectiveness of AST-pretreated MSCs on IRI-AKI mice. Compared with the AKI group, MSCs administration significantly reduced serum creatinine (Scr) and blood urea nitrogen (BUN) levels at 72 h. Notably, Scr and BUN levels in the mice of AST-pretreated MSCs (AST-MSCs) group were even much lower than those in the unpretreated MSCs (MSCs) group (Fig. 1A and B). To determine the severity of renal pathological manifestation, Periodic-Acid Schiff (PAS) staining was performed. Sham mice did not show any significant tubular injury. AKI mice showed tubular brush border loss, cast formation, tubular dilatation, and tubular necrosis, accompanied by increased renal tubular injury scores. MSCs administration reduced the renal histological injury and acute tubular necrosis (ATN) scores caused by IRI. And this effect was more significant in AST-MSCs administration group (Fig. 1C and D).

We also detected the serum levels of the inflammatory cytokines IL-6, IL-10, and TNF-α in mice of different groups. As shown in Fig. 1E–G, mice with AKI injected with either unpretreated or pretreated MSCs led to a considerable decrease in IL-6 and TNF-α levels and an increase in IL-10 level. Furthermore, the AKI mice subjected to AST-pretreated MSCs exhibited lower serum levels of IL-6 and TNF-α and higher levels of IL-10 compared to those subjected to unpretreated MSCs.

AST modulates PGE2 secretion by upregulating PTGS2/COX2

To understand the role of AST on MSCs, we performed RNA sequencing on MSCs stimulated with or without

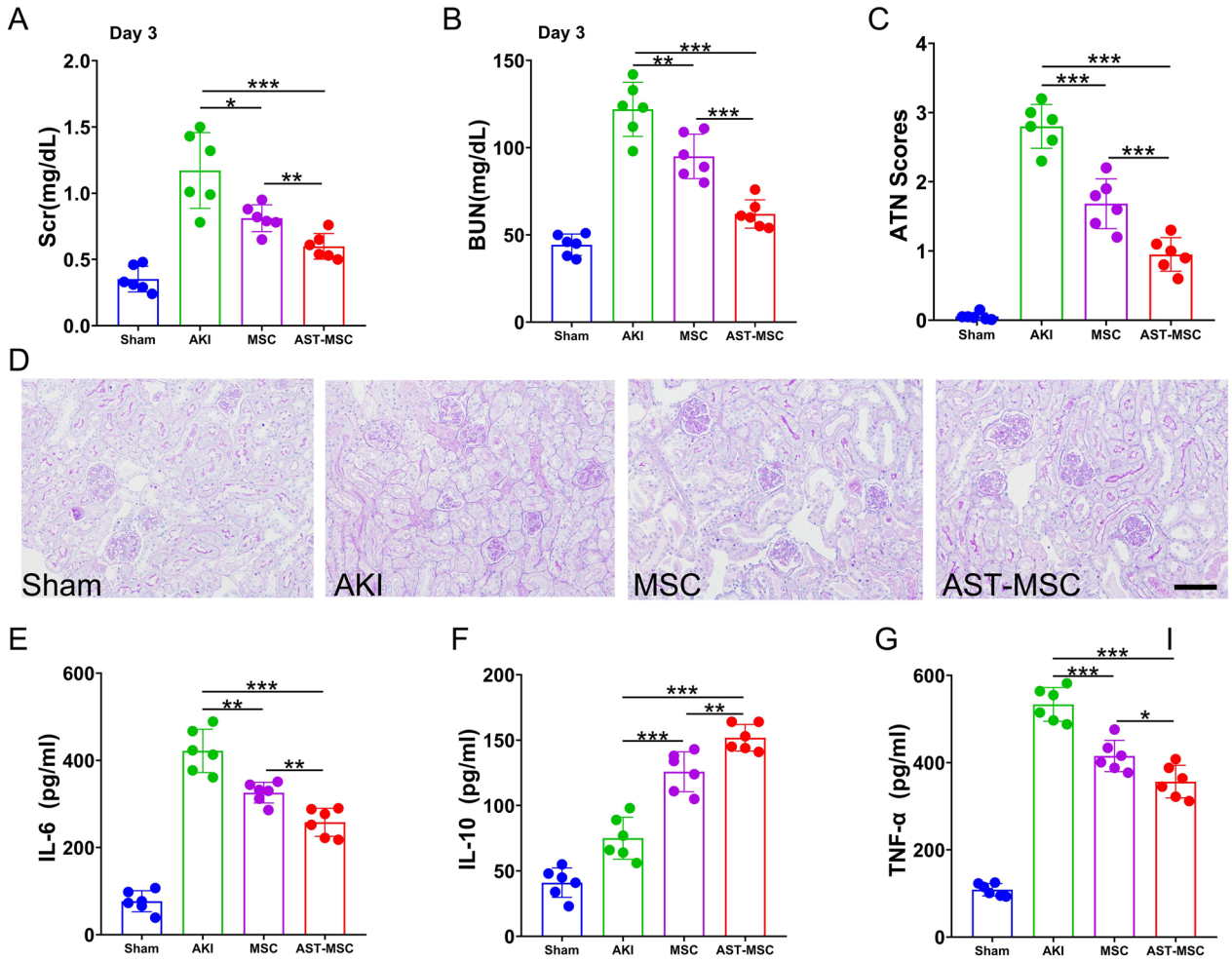

Fig. 1 AST enhanced the therapeutic efficacy of MSCs in attenuating the histological, functional deterioration and decreasing inflammation for AKI. (**A**) Scr and (**B**) BUN were measured on day 3 after reperfusion. (**D**) Periodic acid–Schiff staining(200 × magnification) of the kidney and (**C**) Acute tubular necrosis (ATN) scores at day 3 after reperfusion. Using ELISA, the serum (**E**) IL-6, (**F**) IL-10 and (**G**)TNF-α levels of various mouse groups were evaluated. (scan bar = 100 μm) (n = 6 per group; *$p < 0.05$, **$p < 0.01$, and ***$p < 0.001$)

AST. A total of 2456 differentially expressed genes (DEGs) were discovered between the AST pretreated and unpretreated groups (Fig. 2A). Then, the DEGs were subjected to GO enrichment and KEGG pathway analysis. The results revealed that the DEGs were mainly involved in cell cycle, cell division, DNA repair and other processes in GO enrichment analysis (Fig. S2), while the majority of DEGs were enriched in DNA replication, cell cycle, IL-17 signaling pathway and cytokine-cytokine receptor interaction in KEGG pathway analysis (Fig. 2B). More importantly, the expression of prostaglandin-endoperoxide synthase 2 (PTGS2), a main functional gene in the IL-17 signaling pathway [20], was showed to be significantly up-regulated (4.08-fold) in MSCs after AST pretreatment. The mRNA level of PTGS2 and the protein level of COX-2 in MSCs as well as the concentration level of PGE2 in MSCs supernatant were measured. The results proved that AST pretreatment significantly increased the expression of PTGS2 and COX-2 in MSCs as well as PGE2 in MSCs supernatant (Fig. 2C–E). Collectively, these findings indicate that AST could enhance the secretion of PGE2 by MSCs via upregulating PTGS2/COX-2.

AST promotes PTGS2 expression by binding with KLF4 in MSCs

As demonstrated above, we found that AST could upregulate COX-2/PGE2 expression in MSCs. Then, the specific molecular mechanism of AST on MSCs was investigated. We identified the direct targets for AST using the DARTS technique. Figure 3A depicted the chemical structure of AST. We incubated MSCs lysates with 20 μg/mL AST at various pronase ratios and observed the most differential protein bands at 40–55 kD in a 1:1000 pronase ratio (Fig. 3B). Then, LC–MS/

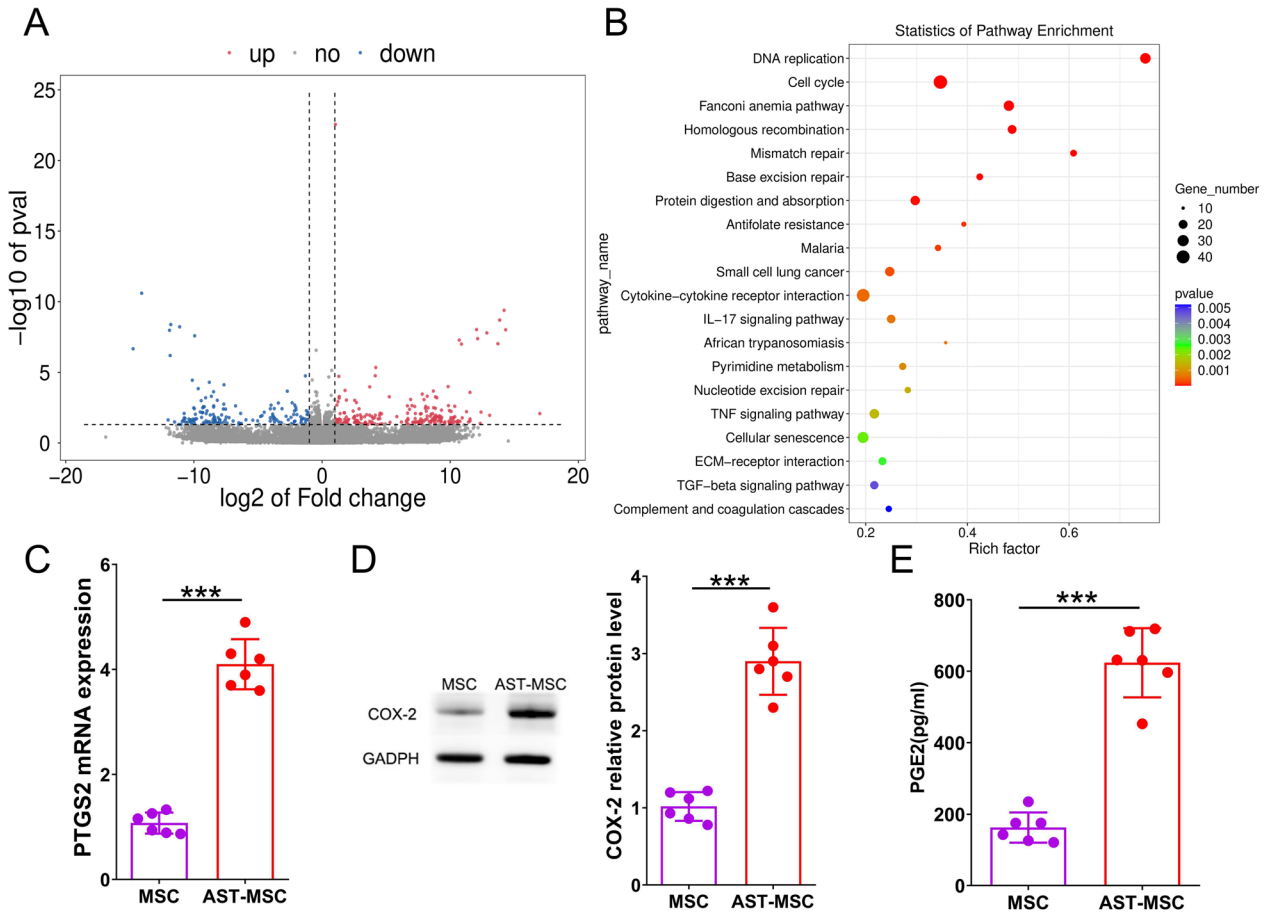

Fig. 2 Bioinformatics analysis of RNA sequencing performed on MSCs that have been treated with AST. Differentially expressed genes (DEGs) can be shown in a plot called a volcano plot (**A**). The genes that have been elevated are represented by red dots, while those that have been downregulated are represented by blue dots. The results of KEGG analysis showed that there was a total of 20 signaling pathways that had the highest enrichment (**B**). Different colors reflect different *p* values, while different circle sizes represent different gene counts. The relative amounts of PTGS2 mRNA(**C**) and COX-2 protein (**D**) in MSCs were determined with the help of RT-PCR and Western blot analysis, respectively. ELISA was utilized to determine the PGE2 content that was present in the supernatant of MSCs(**E**). (n = 6 per group; student t-test, $*p < 0.05$, $**p < 0.01$, $***p < 0.001$). Corresponding uncropped full-length gels and blots are presented in Additional file 1

MS analysis was utilized to find out the unique peptides targeted by AST in the particular gel band. The target protein was chosen based on the number of distinct peptides (> 10), *p*-value (< 0.05), fold change (> 1.2) and literature searching. The final screening results were shown in Table 1. We focused primarily on transcription factor proteins because they play a crucial role in regulating gene expression under various conditions. Among these proteins, KLF4 had the most significant difference with a p-value less than 0.001.

To validate the combination of AST and KLF4, Autodock Vina for molecular docking was employed. The PDB ID for KLF4 in RCSB PDB database is 6vtx. The docking prediction results revealed that the molecular docking energy score of KLF4-AST was −6.9 kcal/mol. Figure 3C displayed the molecular docking binding pattern diagram of KLF4 and AST. Overall, these analyses suggest that

(See figure on next page.)

Fig. 3 KLF4, the target for AST, directly binds the PTGS2 promoter to promote its expression in MSCs. (**A**) Chemical structure of AST. (**B**) the DARTS assay detecting a marked increase in the 40–55 kD band following MSCs incubation in pronase-digested MSCs lysates, and (**C**) the molecular docking models of KLF4 and astilbin. (**D**) Real binding of KLF4 with astilbin confirmed by SPR assay. (**E**) Binding motif of KLF4 identified by WebLogo in the JASPAR online tools. (**F**) The PTGS2 promoter region to which KLF4 binds. (**G**) The ChIP-PCR results for PTGS2. (**H**) Dual-luciferase reporter assay results. The data are presented as the mean standard deviation, with $***p < 0.001$

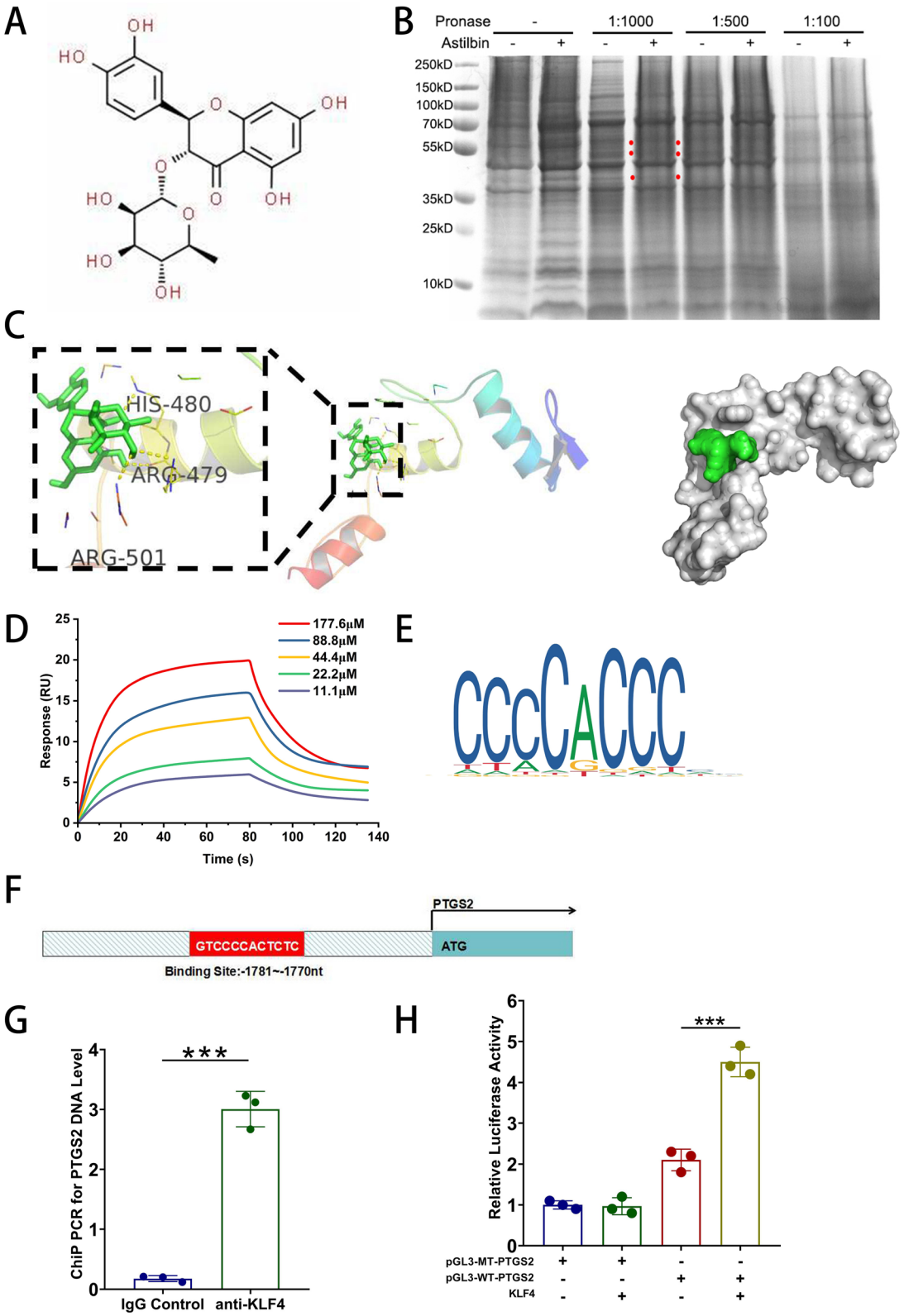

Fig. 3 (See legend on previous page.)

Table 1 Differential proteins screened by the combination of DARTS and LC–MS/MS

Gene name	Peptide number	Fold change	*p* value
KLF4 (54 kDa)	28	1.7	$p < 0.001$
ELK1 (45 kDa)	26	1.4	0.007
ETS1 (50 kDa)	16	1.8	0.003
KLF15 (44 kDa)	14	2.1	0.002
ERG (55 kDa)	22	1.5	0.02

Table 2 Candidate transcription factor of PTGS2-binding predicted by JASPAR

Name	Score	Start	End	Strand	Predicted sequence
MA0039.4.KLF4	9.577425	1770	1781	–	gtccccactctc
MA0028.1.ELK1	8.760425	1819	1828	–	aaatcggaaa
MA1513.1.KLF15	8.6409645	1540	1550	–	ctcccgccgcc
MA0474.2.ERG	8.450432	1117	1126	–	aaaggaagcg
MA0098.1.ETS1	7.7971845	1668	1673	–	cttccg

AST could bind to KLF4 in MSCs. Recombinant KLF4 protein was used to detect the interaction with astilbin by SPR assay. KLF4 stably docked astilbin with a dissociation rate (K_D) of 48.9 (μM) (Fig. 3D).

The above experiments showed that AST pretreatment significantly increased PTGS2 mRNA levels in MSCs. Therefore, we further searched for PTGS2 binding elements in the 3'-enhancer region using JASPAR, an online database for transcription factor binding profiles (http://jaspar.genereg.net/) to ascertain whether there is a KLF4 binding site in the promoter region of PTGS2. The JASPAR scores of the transcription factor proteins screened by DARTS were calculated and the results were presented in Table 2. We discovered that the predicted JASPAR score of KLF4 was 9.577, indicating that it might be the predominant transcription factor for PTGS2. The JASPAR online tools also revealed that KLF4 contains three C2H2 zinc fingers (Fig. 3E) and the promoter sequence of PTGS2 contains a C2H2 zinc finger factor motif at $-1781 \sim -1770$ nt (5′-GTCCCCACTCTC-3′) (Fig. 3F), suggesting that PTGS2 might be the target of KLF4.

To further verify the targeting relationship between PTGS2 and KLF4, dual-luciferase reporter gene assay in conjunction with ChIP-PCR were utilized. The results of ChIP-PCR showed that anti-KLF4 antibody group had higher level of PTGS2 expression than that of the control group, confirming that KLF4 could bind to the PTGS2 promoter (Fig. 3G). In addition, we found that the wild-type PTGS2 promoter group of MSCs displayed more luciferase activity than the pGL3 vector group and the mutant group. This promoter activity was increased by KLF4 overexpression and could be reversed through transfection with a plasmid expressing the mutant promoter region (Fig. 3H). Collectively, these data suggest that PTGS2 appeared to be a direct transcriptional target of KLF4.

AST-pretreated MSCs promote a change in the phenotype of macrophages to M2 by increasing the secretion of PGE2

As described above, AST pretreatment not only significantly increased the mRNA level of PTGS2 and the protein level of COX2 in MSCs, but also increased the level of PGE2 in the MSCs supernatants. Previous studies have reported that MSCs exert their anti-inflammatory effects partially through the secretion of PGE2 and PGE2 influences boosting the polarization of macrophages toward M2 phenotype [21]. Thus, we then investigated whether AST pretreated MSCs would affect the phenotypic change of macrophages in RAW264.7 cells. To examine this, we cocultured AST-pretreated MSCs with RAW264.7 cells and measured the expression of CD163, CD206, and F4/80 after 48 h. There was no significant difference in F4/80 protein levels. Nevertheless, the protein levels of CD163 and CD206 were upregulated after coculture in AST-pretreated MSCs group compared to those in the unpretreated group, indicating that the polarization of RAW264.7 cells towards M2-like macrophages was induced (Fig. 4A–E).

Based on the above results, we hypothesized that AST pretreatment improved the efficacy of MSCs by converting macrophages into M2 phenotype through PTGS2/PGE2 pathway. To test this hypothesis, first, we transfected MSCs with shRNA-PTGS2 or negative control shRNA (shRNA-NC) for 12 h and then treated them with 20 μg/mL AST for another 48 h. Compared to those transfected with shRNA-NC, MSCs transfected with shRNA-PTGS2 exhibited a significant decrease in PTGS2 mRNA and PGE2 supernatant expression(Fig. 4F–G). Next, we cocultured RAW264.7 cells with those transfected MSCs to determine the effect of shRNA-PTGS2 on macrophage phenotypic change. The protein level of CD163 was increased in AST-pretreated MSCs transfected with shRNA-NC, whereas this upregulation effect was not observed in AST-pretreated MSCs transfected with shRNA-PTGS2 (Fig. 4H–J). These results indicated that knockdown of PTGS2 reversed the ability of AST-pretreated MSCs in altering macrophage polarization toward M2 phenotype.

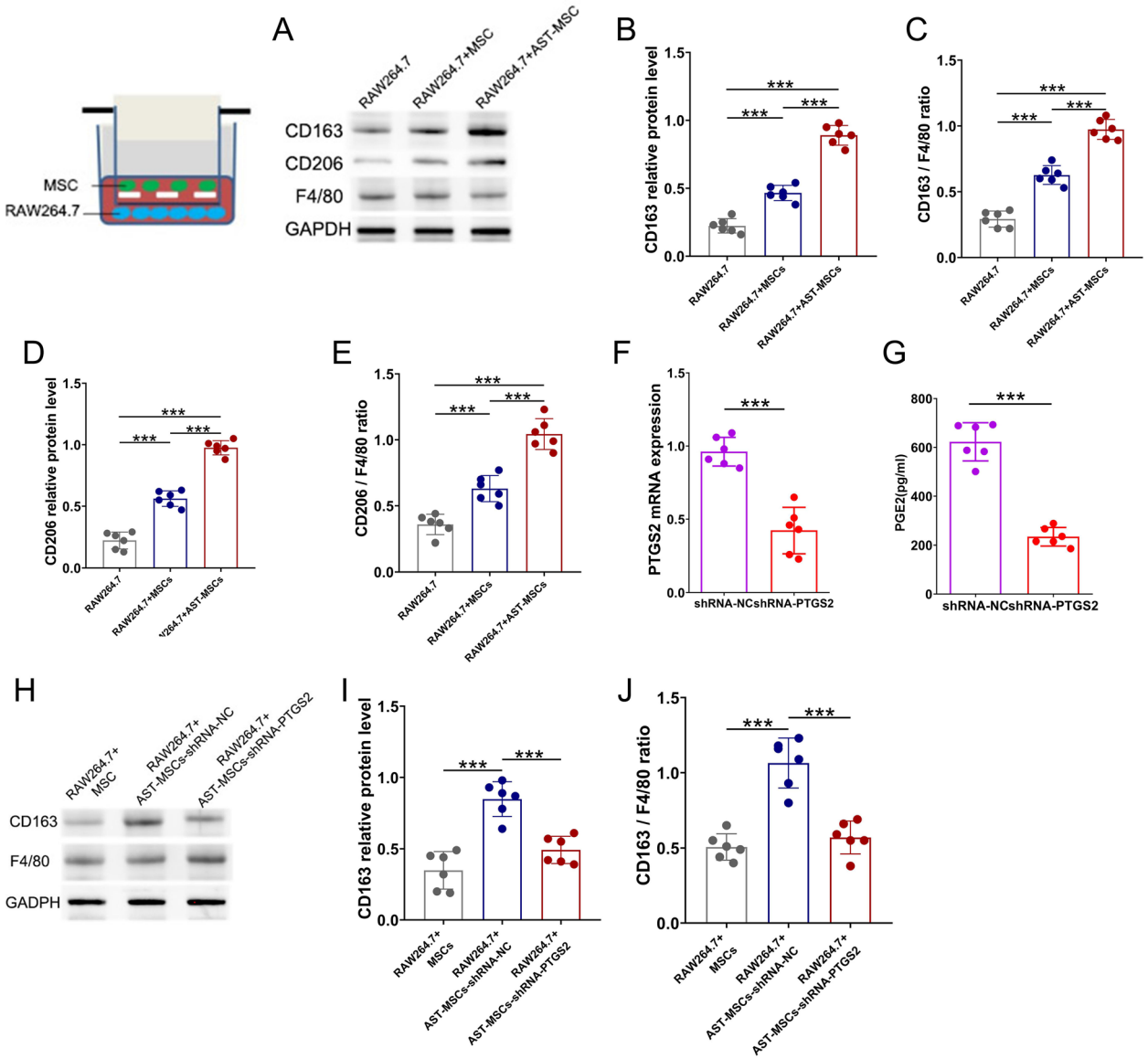

Fig. 4 AST-pretreated MSCs promote a change in the phenotype of macrophages to M2 by increasing the secretion of PGE2. (**A**–**E**) CD163 and CD206 protein expression in RAW264.7 cells after co-cultured MSCs or astilbin (AST) pretreated MSCs. (A)Western blot analysis showing the expression of CD163, CD206 and F4/80. Phenotypic changes of RAW264.7 cells were evaluated by CD163 (**B** and **C**) and CD206 (**D** and **E**) protein levels. CD163 and CD206 protein levels were normalized to the GAPDH and F4/80 levels. The levels of PTGES mRNA (**F**) and PGE2 (**G**) in supernatants were measured using real-time PCR and ELISA, respectively. (**H**–**J**) Astilbin-treated MSCs transfected with shRNA-NC increased CD163 protein levels, whereas astilbin-treated MSCs transfected with shRNA-PTGS2 reversed this upregulation. (n = 6 in each group $^{*}p < 0.05$; $^{***}p < 0.001$) Corresponding uncropped full-length gels and blots are presented in Additional file 1

Knockdown of PTGS2 blocked the efficacy of AST-MSCs on AKI and AKI-CKD

To verify that AST enhanced the therapeutic efficacy of MSCs through PTGS2-mediated pathway in vivo, we administered shRNA-PTGS2 transfected AST-pretreated MSCs into the AKI and AKI-CKD mice models. As anticipated, a significant decrease in Scr, BUN and ATN scores were observed in AST-pretreated MSCs mice group on Day 3 compared with the unpretreated control. However, these effects were diminished when AST-pretreated MSCs were transfected with shRNA-PTGS2 (Fig. 5A–C). The serum levels of the inflammatory cytokines IL-6, TNF-α, and IL-10 were also measured on Day 3 in mice undergoing different treatments. Administration of AST-pretreated MSCs markedly decreased the IL-6 and TNF-αlevels and increased the IL-10 levels in AKI mice,

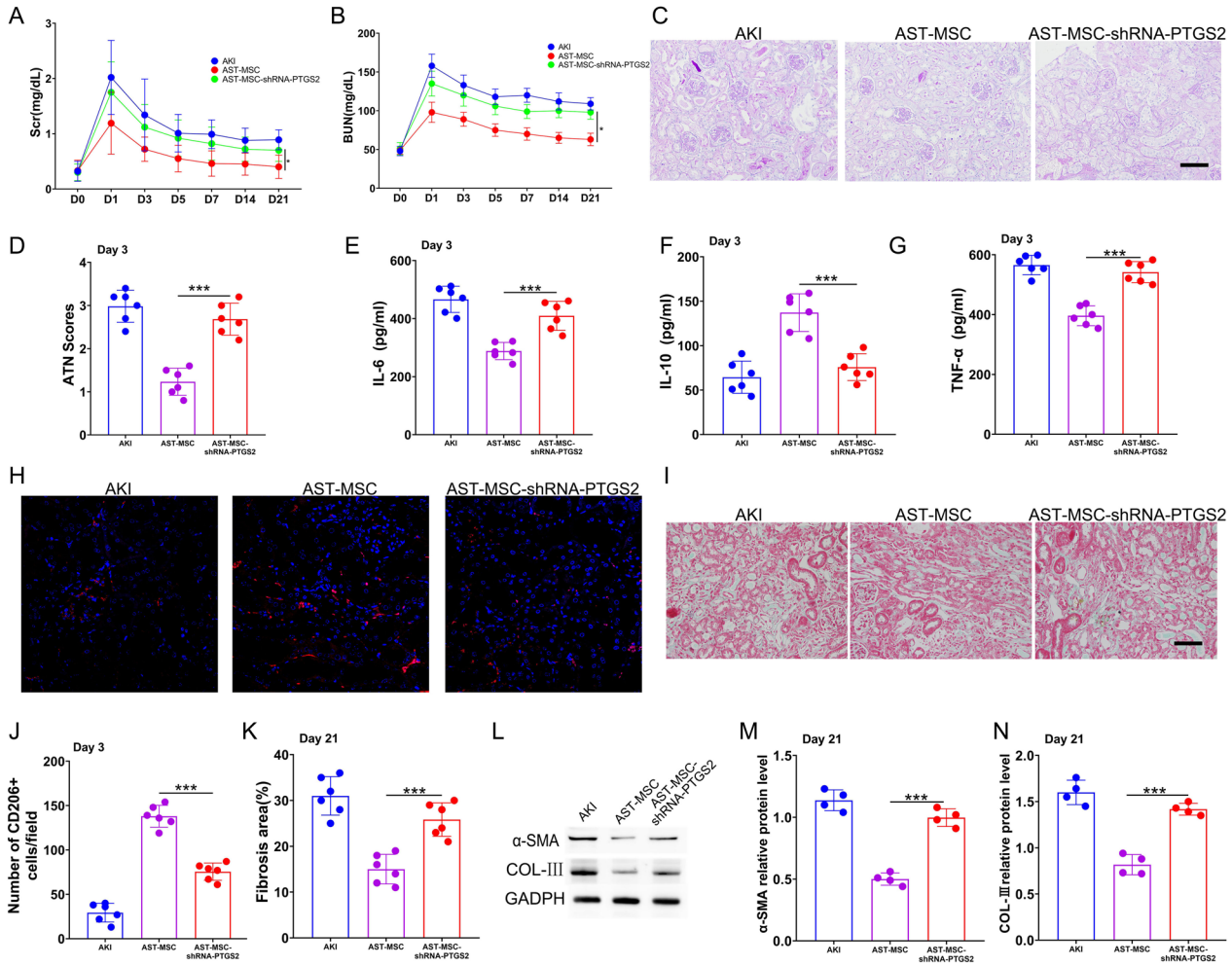

Fig. 5 ShRNA-PTGS2 reverses the enhanced therapeutic efficacy of astilbin-pretreated MSCs in a mouse model of AKI-CKD. (**A**, **B**) Scr and BUN in mice from different groups. (**C**,**D**) PAS staining for kidney Sects. (200 × magnification) and ATN scores. (**E**) IL-6, (**F**) IL-10, (**G**) TNF-α in Serum and (**H**,**J**) immunofluorescence staining of CD206 in kidneys of AKI mice treated on Day 3 with MSCs, astilbin-pretreated MSCs, and shRNA-PTGS2 transfected astilbin-pretreated MSCs. (**I**,**K**)Masson staining in various mouse treatment groups. (**L**,**M**,**N**) On Day 21, the expression of α-SMA and COL-III in the kidneys of distinct mice groups was detected using Western blotting. (scan bar = 100 μm) (The data are shown as the mean standard deviation for n = 3–6 samples. *$p < 0.05$, **$p < 0.01$, ***$p < 0.001$) Corresponding uncropped full-length gels and blots are presented in Additional file 1

whereas these anti-inflammatory effects were reversed by shRNA-PTGS2 transfection (Fig. 5E–G). Consistent with these findings, there was an increased number of CD206 + M2 macrophages in mice treated with AST-pretreated MSCs on Day 3, which was also attenuated when MSCs were transfected with shRNA-PTGS2 (Fig. 5H and J).

Since renal fibrosis is the final common pathway of nearly all progressive kidney diseases [22], we next examined whether PTGS2 blockade would alter the therapeutic potential of MSCs in mitigating renal fibrosis in AKI-CKD models. Masson's trichrome staining was performed and α-SMA and COL-III protein levels were measured in the late-phase treatment on Day 21. A markable decrease in the renal fibrosis scores (Fig. 5 I and K) as well as α-SMA and COL-III (Fig. 5L–N) protein expression were observed, while blockade of PTGS2 abrogated these anti-fibrotic effects. Taken together, these findings indicate that AST potentiates the efficiency of MSCs through PTGS2-mediated pathway.

Discussion

In our present study, we demonstrated that AST pretreatment enhanced the efficacy of MSCs on improving the renal function and pathological presentation in AKI and AKI-CKD mice. And found that the possible

molecular mechanism is AST pretreatment could promote the M2-type polarisation of macrophages through activating of PTGS2-mediated signaling in MSCs.

MSCs have attracted much attention for their ability to regulate inflammatory processes by promoting damaged tissues to form a balanced inflammatory [23]. Many types of innate immune cells, such as macrophages, neutrophils, dendritic cells and natural killer (NK) cells can be regulated by MSCs [24]. MSCs possess the ability to sense environmental alteration and actively alter their epigenetic landscapes and corresponding functions. MSCs can be pre-activated to achieve the desired function and reverse their inactivation because they can recognize the stimuli in the microenvironment and remember them [25]. Several studies have shown that pretreatment with infammatory cytokines and chemical compounds could enhance the immunomodulatory functions of MSCs and their potential therapeutic efficiencies. Pretreatment of MSCs with IFNγ or IFNγ combined with IL-1 or TNF increased the efficacy of MSCs in animal models of DTH, liver injury, colitis, GvHD, arthritis and acute ischaemia [26–29],suggesting that manipulation of MSCs before infusion increases their therapeutic efficacy.

AST is an active natural compound, which can be found in various food and medical plants. AST was found to affecting the immune system extensively by acting on various immunomodulators and inflammatory modulators [30–32]. Several researches have demonstrated that AST could alleviate tissue injury through its immunomodulatory effects. AST attenuated the symptoms of autoimmune myasthenia gravis model by inhibiting Th17 cytokines and up-regulating T regulatory cells [33]. AST could also inhibit the inflammation in glomerular mesangial cells caused by high glucose via NF-κB pathway [34]. Compared with simple cytokine stimulation, AST possesses various benificial pharmacological like anti-inflammatory activity, antimicrobial activity, and antioxidative action etc. [14]. AST could suppress the generation of nitric oxide and TNF-α in RAW 264.7 cells [35]. AST, as an antioxidant, could alleviate DON-induced IPEC-J2 cell toxicity and inflammation [36]. AST is also believed to play an antioxidant role in MSCs [15]. AST might be effective in improving the efficiency of MSCs through modulating the microenvironment generated by ischemic injury. Taking the advantage of AST's various pharmacological properties, we used AST-pretreated MSCs to treat in AKI and AKI-CKD mouse model.

According to GO and KEGG pathway enrichment analysis, we identified a PTGS2-mediated pathway as the key signaling pathway in MSCs after AST pretreatment. PTGS2, a main functional gene in the IL-17 signaling pathway [20] encodes the protein cyclooxygenase-2 (COX-2), which converts arachidonic acid (AA) into prostaglandin E2 (PGE2) [37]. To investigate how AST promotes the expression of PTGS2 in MSCs, we identified the potential candidates that interacts with AST using the DARTS method [38]. And the result indicated that AST can bind to KLF4. Molecular docking also showed AST could bind with KLF4 protein. KLF4 is a transcription factor plays a key role in self-renewal and maintenance of the undifferentiated state in stem cells [39]. KLF4 is also one of the four original iPSC reprogramming factors [40]. It acts as a repressor of somatic-specific genes and as a pioneer factor to activate epigenetically suppressed pluripotency genes during early reprogramming. It also acts as an activator of pluripotency genes by binding to super-enhancers of pluripotency factors to facilitate long-range interactions among pluripotency factor binding sites [41]. At the same time, combined with JASPAR database for transcription factor binding predictions, we found that KLF4 is also a suitable upstream transcription factor for PTGS2. We validated PTGS2 as KLF4's direct transcriptional target using ChIP-PCR and luciferase assays. AST increases the expression of PTGS2, which binds to KLF4 and induces MSCs to secrete PGE2. Based on these novel techniques, we explain the specific protein binding sites and possible mechanisms of AST promotes the expression of PTGS2 in MSCs.

Our study examined the immunoregulatory capacity of AST-pretreated MSCs and the results indicated that the administration of AST-pretreated MSCs down-regulated the expression of the inflammation markers in the injured kidneys. In addition, the renal function, renal pathological changes and the expression of fibrosis-related protein were significant decreased in AST-pretreated MSCs group compared with the unpretreated MSCs group. According to our study, MSCs treated with AST produced more PGE2, resulting in a more pronounced polarization of M2 macrophages in vitro. M2 macrophages play a vital role in the progression of renal fibrosis and inflammation. In the acute phase of inflammation, M2 macrophages secrete growth factors to aid in the repair of kidney damage. Our study showed that AST-pretreated MSCs significantly increased the number of CD206 + M2 macrophages on Day 3 after AKI in mice. In mice with AKI-CKD, the knockdown of PTGS2 diminished the anti-inflammatory and anti-fibrotic effects of MSCs treated with AST. These findings indicated that MSCs pretreated with AST exert intrinsic reparative properties through polarizing macrophages to an M2 phenotype. PGE2 and M2 macrophages played significant roles in the immunosuppressive effect of AST-treated MSCs.

There are also several limitations in the study. Firstly, Vitro screening by DARTS technology may not provide

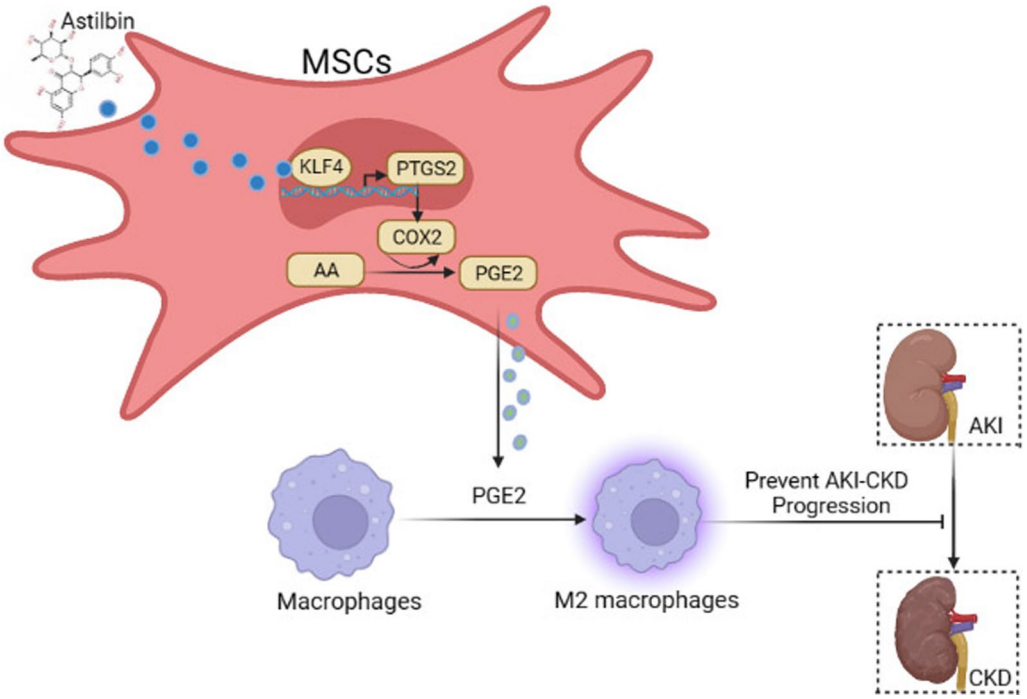

Fig. 6 Schematic illustration depicting the mechanism of AST-pretreated MSCs treat AKI-CKD. By binding with the transcription factor KLF4 in MSCs, astilbin promotes the expression of PTGS2/COX2, enhances the transformation of AA to PGE2, promotes the M2-type polarisation of macrophages, and ultimately increases the efficacy of MSCs on AKI-CKD mice (This picture is created in BioRender)

absolutely accurate results. Some low abundant proteins might not be discovered because their positive spots are easily omitted in the mass spectrometry analysis. In addition, due to the complexity of protein libraries, some erroneous binding between small molecules and proteins may be captured during routine operations. Secondly, we investigated the expressions of PTGS2 and the related molecules in MSCs after AST pretreatment in vitro but didn't detect other molecules that expressed significant changes. Therefore, the results could not be comprehensively integrated. Thirdly, due to the absence of necessary resources, this study only examined the changes in PTGS2-mediated pathway related genes after AST pretreatment without their associated molecular mechanisms, which shall be explored in the future. In addition, the findings of a murine study may not necessarily apply to humans, and there are differences between human and mouse MSCs and macrophages. Moreover, further experiments need to be conducted to address the above issues and to clarify the different expressed genes in AST pretreatment and the underlying molecular mechanisms.

Conclusions

In summary, our study demonstrates a new therapeutic application of MSCs in the treatment of AKI and AKI-CKD. MSCs pretreated with AST showed a better therapeutic efficacy than untreated MSCs. We observed MSCs pretreated with AST could significantly ameliorate AKI and AKI-CKD in mouse model via PGE2, which polarizes M2 macrophages. Additionally, AST appears to bind KLF4 and then promote MSCs through improving the PTGS2-mediated pathway (Fig. 6). Overall, AST pretreatment may be a promising strategy to enhance the therapeutic potential of MSCs in the treatment of kidney diseases. This approach provides a novel avenue for the effective application of MSCs treatment.

Supplementary Information

The online version contains supplementary material available at https://doi.org/10.1186/s13287-024-04025-3.

Additional file 1.
Additional file 2.
Additional file 3.
Additional file 4.
Additional file 5.

Acknowledgements
The authors declare that they have not used Artificial Intelligence in this study.

Author contributions
QH, GYC, HJH and XMC conceived and designed the experiments. XDG, ZNF, KC, CL, and GRG performed the experiments. ZNF and XDG analyzed the data

and wrote the manuscript. QH revised the manuscript. QH, HJH, CL and XDG provided funding. The authors read and approved the final manuscript.

Funding
This work was supported by National Natural Science Foundation of China (No. 82204744, 82270758, 82070741 and 82200780) and China Postdoctoral Science Foundation (2022M723899), Shanghai Songjiang District Scientific and Technological Project (2023SJKJGG054 to Haijuan Hong).

Availability of data and materials
The authors confirm that the data supporting the findings of this study are available within the article and its supplementary materials.

Declarations

Ethics approval and consent to participate
All animal experiments were conducted in accordance with the ARRIVE guidelines 2.0 (Animal Research: Reporting of In Vivo Experiments) and approved by the by the Ethics Committee for the Use of Animals of PLA General Hospital. (Approval No. 2022-X18-36, "Astilbin improves the therapeutic effects of mesenchymal stem cells in AKI-CKD mice by regulating macrophage polarization through PTGS2-mediated pathway" approved on November 5, 2022). Human bone marrow MSCs were obtained from Cyagen Company (Guangzhou, China). Cyagen Company has confirmed that there was initial ethical approval for collection of human cells, and that the donors had signed informed consent.

Consent for publication
All authors confirm their consent for publication.

Competing interests
The authors declare that they have no competing interests.

Author details
[1]Department of Nephrology, First Medical Center of Chinese PLA General Hospital, Nephrology Institute of the Chinese PLA, State Key Laboratory of Kidney Diseases, National Clinical Research Center for Kidney Diseases, Beijing Key Laboratory of Kidney Disease Research, Beijing 100853, China. [2]Medical School of Chinese PLA, Beijing 100853, China. [3]Healthcare Office of Service Bureau, Agency for Offices Administration, Central Military Commission, People's Republic of China, Beijing 100034. [4]Department of Critical Care Medicine, 920th Hospital of Joint Logistics Support Force of Chinese PLA, Kunming 650032, Yunnan Province, China. [5]Department of Critical Care Medicine, First Medical Center of Chinese PLA General Hospital, Beijing 100853, China. [6]Department of Nephrology, Shanghai Songjiang District Central Hospital, Shanghai 201600, China.

Received: 26 July 2024 Accepted: 28 October 2024
Published online: 14 November 2024

References

1. Choi ME. Autophagy in kidney disease. Annu Rev Physiol. 2020;82:297–322.
2. Zhu H, Cao C, Wu Z, Zhang H, Sun Z, Wang M, Xu H, Zhao Z, Wang Y, Pei G, et al. The probiotic L. casei Zhang slows the progression of acute and chronic kidney disease. Cell Metab. 2021;33(10):1926–42.
3. Yun CW, Lee SH. Potential and therapeutic efficacy of cell-based therapy using mesenchymal stem cells for acute/chronic kidney disease. Int J Mol Sci. 2019;20(7):1619.
4. Fazekas B, Griffin MD. Mesenchymal stromal cell-based therapies for acute kidney injury: progress in the last decade. Kidney Int. 2020;97(6):1130–40.
5. Marcheque J, Bussolati B, Csete M, Perin L. Concise reviews: stem cells and kidney regeneration: an update. Stem Cells Transl Med. 2019;8(1):82–92.
6. Liao C, Chen G, Yang Q, Liu Y, Zhou T. Potential therapeutic effect and mechanisms of mesenchymal stem cells-extracellular vesicles in renal fibrosis. Front Cell Dev Biol. 2022;10: 824752.
7. Zhou X, Hong Y, Zhang H, Li X. Mesenchymal stem cell senescence and rejuvenation: current status and challenges. Front Cell Dev Biol. 2020;8:364.
8. Han YS, Kim SM, Lee JH, Jung SK, Noh H, Lee SH. Melatonin protects chronic kidney disease mesenchymal stem cells against senescence via PrPC-dependent enhancement of the mitochondrial function. J Pineal Res. 2019;66(1):e12535.
9. Altun B, Yilmaz R, Aki T, Akoglu H, Zeybek D, Piskinpasa S, Uckan D, Purali N, Korkusuz P, Turgan C. Use of mesenchymal stem cells and darbepoetin improve ischemia-induced acute kidney injury outcomes. Am J Nephrol. 2012;35(6):531–9.
10. Bai M, Zhang L, Fu B, Bai J, Zhang Y, Cai G, Bai X, Feng Z, Sun S, Chen X. IL-17A improves the efficacy of mesenchymal stem cells in ischemic-reperfusion renal injury by increasing Treg percentages by the COX-2/PGE2 pathway. Kidney Int. 2018;93(4):814–25.
11. Ahmadifard R, Jafarzadeh A, Mahmoodi M, Nemati M, Rahmani M, Khoramdelazad H, Ayoobi F. Interferon-gamma-treated mesenchymal stem cells modulate the T cell-related chemokines and chemokine receptors in an animal model of experimental autoimmune encephalomyelitis. Drug Res (Stuttg). 2023;73(4):213–23.
12. Xu H, Fu J, Chen L, Zhou S, Fang Y, Zhang Q, Chen X, Yuan L, Li Y, Xu Z, et al. TNF-alpha enhances the therapeutic effects of MenSC-derived small extracellular vesicles on inflammatory bowel disease through macrophage polarization by miR-24-3p. Stem Cells Int. 2023;2023:2988907.
13. Yang D, Zhang QF. The natural source, physicochemical properties, biological activities and metabolism of astilbin. Crit Rev Food Sci Nutr. 2023;63(28):9506-9518.
14. Sharma A, Gupta S, Chauhan S, Nair A, Sharma P. Astilbin: a promising unexplored compound with multidimensional medicinal and health benefits. Pharmacol Res. 2020;158: 104894.
15. Liu J, Li X, Lin J, Li Y, Wang T, Jiang Q, Chen D. Sarcandra glabra (Caoshanhu) protects mesenchymal stem cells from oxidative stress: a bioevaluation and mechanistic chemistry. BMC Compl Altern Med. 2016;16(1):423.
16. Burley SK, Kurisu G, Markley JL, Nakamura H, Velankar S, Berman HM, Sali A, Schwede T, Trewhella J. PDB-Dev: a prototype system for depositing integrative/hybrid structural models. Structure. 2017;25(9):1317–8.
17. Eberhardt J, Santos-Martins D, Tillack AF, Forli S. AutoDock Vina 1.2.0: new docking methods, expanded force field, and python bindings. J Chem Inf Model. 2021;61(8):3891–8.
18. Trott O, Olson AJ. AutoDock Vina: improving the speed and accuracy of docking with a new scoring function, efficient optimization, and multithreading. J Comput Chem. 2010;31(2):455–61.
19. Wu L, Li O, Zhu F, Wang X, Chen P, Cai G, Chen X, Hong Q. Krupsilonppel-like factor 15 suppresses renal glomerular mesangial cell proliferation via enhancing P53 SUMO1 conjugation. J Cell Mol Med. 2021;25(12):5691–706.
20. Qin C, Wu M, Wang X, Zhang W, Qi G, Wu NY, Liu X, Lu Y, Zhang J, Chai Y. Study on the mechanism of Danshen-Guizhi drug pair in the treatment of ovarian cancer based on network pharmacology and in vitro experiment. PeerJ. 2022;10: e13148.
21. Fontaine MJ, Shih H, Schafer R, Pittenger MF. Unraveling the mesenchymal stromal cells' paracrine immunomodulatory effects. Transfus Med Rev. 2016;30(1):37–43.
22. Djudjaj S, Boor P. Cellular and molecular mechanisms of kidney fibrosis. Mol Aspects Med. 2019;65:16–36.
23. Markov A, Thangavelu L, Aravindhan S, Zekiy AO, Jarahian M, Chartrand MS, Pathak Y, Marofi F, Shamlou S, Hassanzadeh A. Mesenchymal stem/stromal cells as a valuable source for the treatment of immune-mediated disorders. Stem Cell Res Ther. 2021;12(1):192.
24. Li H, Dai H, Li J. Immunomodulatory properties of mesenchymal stromal/stem cells: the link with metabolism. J Adv Res. 2023;45:15–29.
25. Meirong L, Yufeng J, Qian H, Yali Z, Lingzhi Z, Xiaobing F: Potential preactivation strategies for improving therapeutic efficacy of mesenchymal stem cells: current status and future prospects. Stem Cell Res Therapy 2022;13(1).
26. Szabo E, Fajka-Boja R, Kriston-Pal E, Hornung A, Makra I, Kudlik G, Uher F, Katona RL, Monostori E, Czibula A. Licensing by inflammatory cytokines abolishes heterogeneity of immunosuppressive function of mesenchymal stem cell population. Stem Cells Dev. 2015;24(18):2171–80.

27. Duijvestein M, Wildenberg ME, Welling MM, Hennink S, Molendijk I, van Zuylen VL, Bosse T, Vos AC, de Jonge-Muller ES, Roelofs H, et al. Pretreatment with interferon-gamma enhances the therapeutic activity of mesenchymal stromal cells in animal models of colitis. Stem cells. 2011;29(10):1549–58.
28. Luo Y, Wang Y, Poynter JA, Manukyan MC, Herrmann JL, Abarbanell AM, Weil BR, Meldrum DR. Pretreating mesenchymal stem cells with interleukin-1beta and transforming growth factor-beta synergistically increases vascular endothelial growth factor production and improves mesenchymal stem cell-mediated myocardial protection after acute ischemia. Surgery. 2012;151(3):353–63.
29. Polchert D, Sobinsky J, Douglas G, Kidd M, Moadsiri A, Reina E, Genrich K, Mehrotra S, Setty S, Smith B, et al. IFN-gamma activation of mesenchymal stem cells for treatment and prevention of graft versus host disease. Eur J Immunol. 2008;38(6):1745–55.
30. Hua S, Zhang Y, Liu J, Dong L, Huang J, Lin D, Fu X. Ethnomedicine, phytochemistry and pharmacology of smilax glabra: an important traditional chinese medicine. Am J Chin Med. 2018;46(2):261–97.
31. Liang G, Nie Y, Chang Y, Zeng S, Liang C, Zheng X, Xiao D, Zhan S, Zheng Q. Protective effects of Rhizoma smilacis glabrae extracts on potassium oxonate- and monosodium urate-induced hyperuricemia and gout in mice. Phytomedicine. 2019;59: 152772.
32. Wang SW, Xu Y, Weng YY, Fan XY, Bai YF, Zheng XY, Lou LJ, Zhang F. Astilbin ameliorates cisplatin-induced nephrotoxicity through reducing oxidative stress and inflammation. Food Chem Toxicol. 2018;114:227–36.
33. Zhang J, Liu H, Song C, Zhang J, Wang Y, Lv C, Song X. Astilbin ameliorates pulmonary fibrosis via blockade of Hedgehog signaling pathway. Pulm Pharmacol Ther. 2018;50:19–27.
34. Chen F, Zhu X, Sun Z, Ma Y. Astilbin inhibits high glucose-induced inflammation and extracellular matrix accumulation by suppressing the TLR4/MyD88/NF-kappaB pathway in rat glomerular mesangial cells. Front Pharmacol. 2018;9:1187.
35. Lu CL, Zhu YF, Hu MM, Wang DM, Xu XJ, Lu CJ, Zhu W. Optimization of astilbin extraction from the rhizome of smilax glabra, and evaluation of its anti-inflammatory effect and probable underlying mechanism in lipopolysaccharide-induced RAW264.7 macrophages. Molecules. 2015;20(1):625-644.
36. Xu X, Yan G, Chang J, Wang P, Yin Q, Liu C, Liu S, Zhu Q, Lu F. Astilbin ameliorates deoxynivalenol-induced oxidative stress and apoptosis in intestinal porcine epithelial cells (IPEC-J2). J Appl Toxicol: JAT. 2020;40(10):1362–72.
37. Neuschafer-Rube F, Schon T, Kahnt I, Puschel GP. LDL-dependent regulation of TNFalpha/PGE(2) induced COX-2/mPGES-1 expression in human macrophage cell lines. Inflammation. 2023;46(3):893-911.
38. Pai MY, Lomenick B, Hwang H, Schiestl R, McBride W, Loo JA, Huang J. Drug affinity responsive target stability (DARTS) for small-molecule target identification. Methods Mol Biol. 2015;1263:287–98.
39. Hu S, Metcalf E, Mahat DB, Chan L, Sohal N, Chakraborty M, Hamilton M, Singh A, Singh A, Lees JA, et al. Transcription factor antagonism regulates heterogeneity in embryonic stem cell states. Mol Cell. 2022;82(23):4410–27.
40. Tan JP, Liu X, Polo JM. Establishment of human induced trophoblast stem cells via reprogramming of fibroblasts. Nat Protoc. 2022;17(12):2739–59.
41. Nandan MO, Yang VW. The role of Kruppel-like factors in the reprogramming of somatic cells to induced pluripotent stem cells. Histol Histopathol. 2009;24(10):1343–55.

Publisher's Note